Cell Reports
Methods

Report

iSort enables automated complex microfluidic droplet sorting in an effort to democratize technology

Graphical abstract

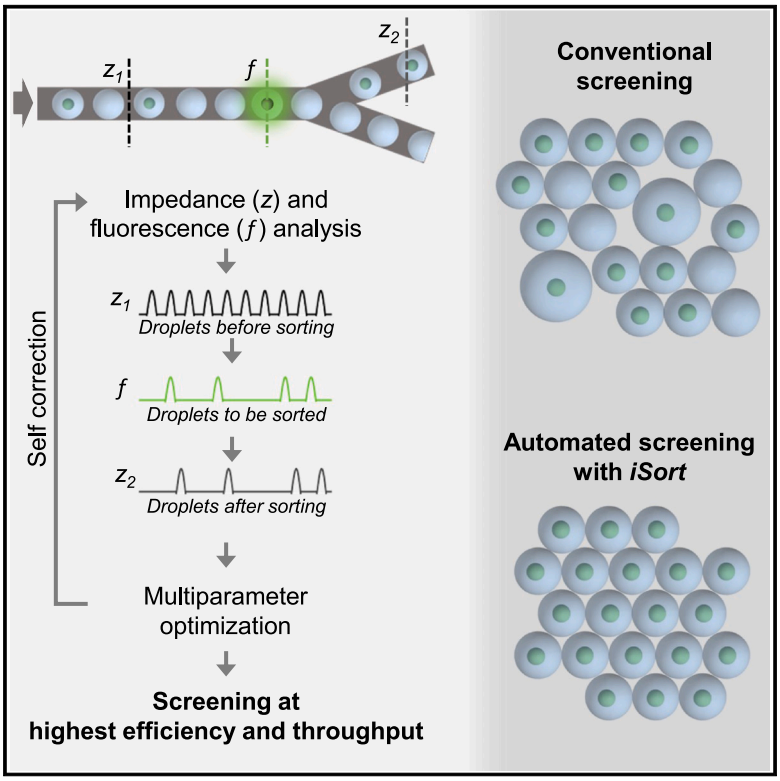

Highlights

- We establish a method to automate high-throughput droplet screening experiments
- The method exploits impedance analysis to improve the screening efficiency in real time
- The method reduces false-positive events even in perturbed and polydispersed conditions

Authors

Jatin Panwar, Ramesh Utharala, Laura Fennelly, Daniel Frenzel, Christoph A. Merten

Correspondence

christoph.merten@epfl.ch

In brief

Panwar et al. establish a method to automate droplet screening in microfluidics. The method monitors the droplet trajectories in real time using impedance analysis to estimate screening efficiency, and it conducts multiparametric optimization to ensure efficient, stable, reproducible, and automated high-throughput droplet screening for phenotypic single-cell analysis.

Panwar et al., 2023, Cell Reports Methods *3*, 100478
May 22, 2023
https://doi.org/10.1016/j.crmeth.2023.100478

CellPress

Cell Reports Methods

CellPress
OPEN ACCESS

Report

iSort enables automated complex microfluidic droplet sorting in an effort to democratize technology

Jatin Panwar,[1,2] Ramesh Utharala,[2] Laura Fennelly,[2] Daniel Frenzel,[2] and Christoph A. Merten[1,2,3,*]
[1]Institute of Bioengineering, School of Engineering, École Polytechnique Fédérale de Lausanne (EPFL), 1015 Lausanne, Switzerland
[2]Genome Biology Unit, European Molecular Biology Laboratory (EMBL), 69117 Heidelberg, Germany
[3]Lead contact
*Correspondence: christoph.merten@epfl.ch
https://doi.org/10.1016/j.crmeth.2023.100478

MOTIVATION Microfluidic droplet sorting has become a powerful tool in high-throughput phenotypic assays at the single-cell level. It has been used for a variety of applications, including antibody discovery, directed evolution, and microbiome screening. However, in contrast to single-cell genomics methods, which are now widely used by labs all over the world, phenotypic single-cell sorting is still somewhat reserved to a small number of highly specialized laboratories. This is due to the complexity of current droplet sorting methods, which are very sensitive to control parameters and require specialized training to acquire the expertise for operating them efficiently. Here, we present a method to overcome this limitation by automating droplet sorting experiments in order to achieve "plug and play" long-term and highly efficient screens.

SUMMARY

Fluorescence-activated droplet sorting (FADS) is a widely used microfluidic technique for high-throughput screening. However, it requires highly trained specialists to determine optimal sorting parameters, and this results in a large combinatorial space that is challenging to optimize systematically. Additionally, it is currently challenging to track every single droplet within a screen, leading to compromised sorting and "hidden" false-positive events. To overcome these limitations, we have developed a setup in which the droplet frequency, spacing, and trajectory at the sorting junction are monitored in real time using impedance analysis. The resulting data are used to continuously optimize all parameters automatically and to counteract perturbations, resulting in higher throughput, higher reproducibility, increased robustness, and a beginner-friendly character. We believe this provides a missing piece for the spreading of phenotypic single-cell analysis methods, similar to what we have seen for single-cell genomics platforms.

INTRODUCTION

High-throughput screening is a critical operation in many drug discovery workflows, facilitating isolation of rare hits from a large non-specific population.[1,2] Fluorescence-activated droplet sorting (FADS) is one such technology that allows sorting of fluorescently labeled biochemical entities encapsulated within droplets at high frequency[3–5] for applications including antibody discovery, directed evolution, and microbiome screening.[6–10] To maintain optimal droplet flow and trajectories over several hours of screening, FADS requires tight control of all parameters. In addition, to sort a droplet, FADS needs a finely tuned high-voltage pulse to generate an electric field that induces a net dielectrophoretic force on the droplet to be sorted, which in turn, modifies the trajectory of that single droplet toward the collection channel.[11] These fluid flow and high-voltage control parameters create a considerably large combinatorial space that needs to be optimized carefully for an efficient screen and that put a significant hurdle for use by non-specialists. With current methods, a typical droplet sorting operation requires manual estimation of all control parameters and verification by checking if the desired droplets end up in the collection channel, using high-speed video recordings capturing only a small section of the operation.[3] In turn, the vast majority of all sorting events cannot be monitored, giving rise to false-positive sorting events due to momentary flow perturbations based on pulsation of the pumps, clogging in microchannels, trapped air bubbles etc. In consequence, sorting of multiple droplets at once or even merging of droplets can occur without being noticed. To overcome these issues and to pave the way for more user-friendly plug and play

devices, we have developed a closed-feedback system, on the basis of impedance-assisted sorting (iSort). It determines the sorting efficiency in real time and systematically iterates the fluid flow and all electrical parameters until the highest efficiency is reached. In addition, the method automatically stops the high-voltage pulse whenever perturbations are detected, resulting in a significant decrease of false-positive events and robust long-term screens without manual intervention.

In contrast to conventional FADS setups, iSort contains dedicated computational and electronic modules to monitor and control the sorting operation (Figure 1A). Briefly, conventional workstations use lasers to excite the fluorophores inside the droplets and collect the emitted light in photomultiplier tubes (PMTs) after spectral separation (Figure 1A). The data from PMTs is acquired and processed in real time by a field programmable gate array (FPGA)-based algorithm and a computer interface is used to define sorting gates, similar to fluorescence-activated cell sorting (FACS) approaches. Finally, the FPGA triggers a high-voltage pulse every time a droplet within the sorting gate passes through the detection zone, resulting in specific collection. The setup typically also includes at least three syringe pumps to deliver continuous phase flow (oil) and dispersed phase flow (aqueous) into the microfluidic chip for droplet generation and to withdraw fluid from the waste channel so that the droplet trajectories are directed toward the waste channel in absence of an electric field (Figures 1A and 1B). Together, the high-voltage pulse and syringe pumps provide the control parameters that need to be optimized and monitored for an efficient long-term sorting, which iSort aims to accomplish computationally. These parameters are the pulse amplitude (A_V), pulse duration (D_V), and pulse delay (L_V), along with the flow rates of continuous phase pump (Q_C), dispersed phase pump (Q_D), and withdrawal pump (Q_W). The purposes and effects of these parameters on sorting efficiency are detailed in Table 1.

To optimize the sorting operation, iSort first needs to acquire the state of the system by detecting droplets and determining their temporal and spatial properties at two points located before and after the sorting operation. The temporal information provides droplet's width (i.e., time taken by the droplet to cross the detection point) and the temporal spacing between two droplets which are used to define the limits and step sizes of the iterations. On the other hand, the two-point measurement ensures that the trajectory of every single droplet is registered, which makes it possible to check if the droplets meant to be sorted are reaching the collection channel or not. This provides the essential information that iSort uses for optimization and for calculating the efficiency of the sorting operation, which in turn reflects the progress of optimization. For droplet detection, our method conducts impedance analysis within microfluidic channels,[12,13] once before the sorting junction and another time in the collection channel. In microfluidics, impedance analysis is commonly used to identify and quantify morphological properties of single cells that are either flowing in a carrier fluid[14–16] or are encapsulated within water-in-oil droplets.[17–20] Such quantification requires extracting signals from an extremely noisy environment using lock-in amplifiers or impedance spectroscopes with multi-frequency excitation.[13,21] However, to derive real-time data on droplet trajectories for the automation of droplet sorting, iSort's algorithm only requires to detect aqueous droplets and not its composition. Droplet's impedance signals are considerably clean because of their larger size and higher permittivity and conductivity of dispersed phase (PBS; permittivity = 80, conductivity = 1.4 Sm^{-1}) compared with carrier phase (fluorinated oil; permittivity = 5.8, conductivity = 10^{-10} Sm^{-1}). Moreover, impedance signals are of same characteristics as the fluorescence signals after being acquired by the PMTs, i.e., one-dimensional voltage signal. As a result, impedance signals can be acquired using the hardware and computational capacity that already exists with the droplet sorting setups[5] (i.e., the FPGA card in addition to a custom made transimpedance amplifier circuit with a single frequency excitation). This way, iSort can be easily integrated with the existing FADS technology for its automation. To measure the droplet impedance, two arrays of platinum microelectrodes were placed before (termed primary impedance electrodes or *Z1*) and after (termed secondary impedance electrodes or *Z2*) the sorting junction (Figure 1B). These electrodes were fabricated by depositing a 200 nm layer of platinum over a 20 nm layer of titanium on a glass substrate, using standard microfabrication methods[12,22] (Figure S1; see STAR Methods for instructions). A polydimethylsiloxane (PDMS) microfluidic chip with embedded high-voltage electrodes used for droplet sorting was also fabricated alongside.[5,23] We bonded the PDMS chip on top of the glass substrate such that *Z1* was orthogonal to the microfluidic channel before the sorting junction and *Z2* was orthogonal to the collection channel (Figure 1C). A coverslip coated with indium tin oxide (ITO) was placed under the glass substrate (ITO side down), which helps in discharging the stray charges developed on the droplets post-sorting.[3–5] A double-sided conductive tape was used to stick the coverslip to the glass substrate such that the ground electrodes of the glass substrate are in electrical connection to the ITO coated side of the coverslip (Figure S1). The complete PDMS-substrate-coverslip assembly was then placed into a three-dimensional (3D) printed holder that has spring loaded connection ports to connect external wires with the electrodes (Figures 1C and 1D). For droplet impedance signal acquisition, the central and a side electrode of *Z1* and *Z2* were excited by a peak-to-peak sinusoidal voltage of 5 V at 10 kHz frequency via a 2-channel function generator and the corresponding voltage change across the central and side electrode due to the droplet's impedance is acquired by the FPGA via a transimpedance amplifier (detailed connections are depicted in Figure S1). After signal processing, a droplet passing over the electrodes appears as a peak in the voltage signal by the virtue of its lower impedance in comparison with the carrier phase (Figure S1). The optimization can be initiated once the droplet signals are identified and the number of droplets before and after the sorting junction at any time interval along with the number of droplets to be sorted in that time are registered by iSort (see STAR Methods for instructions to set up the experiment and initiate iSort). The optimization algorithm works in two modes, scanning mode and screening mode (Figure S2). In scanning mode, the algorithm tries to find the best configurations for a given microfluidic chip and this configuration is then used as initial values in screening mode. This two-mode iSort operation ensures that when the same chip is used for actual screening

CellPress
OPEN ACCESS

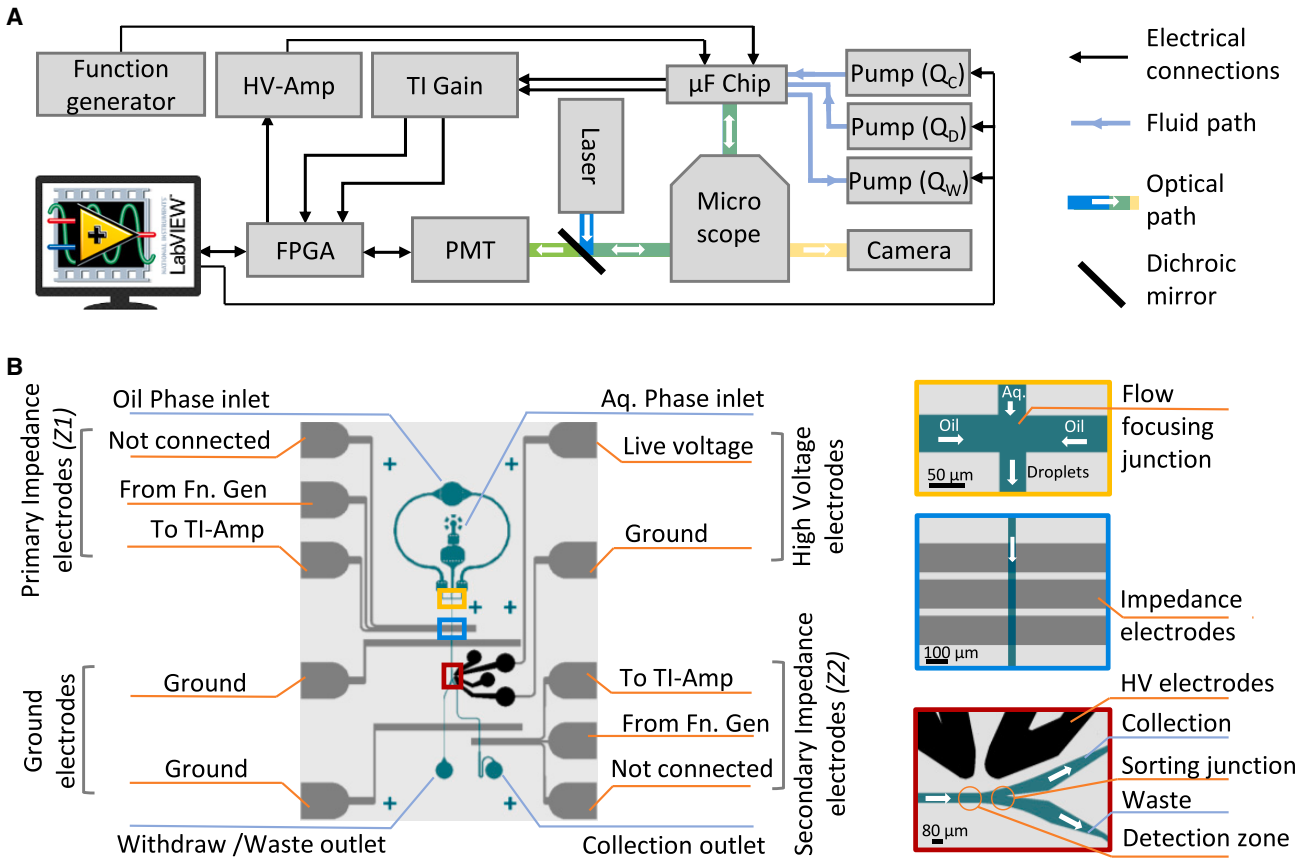

Figure 1. iSort setup

(A) Schematic of the setup. A microfluidic (microfarad) chip is placed over a microscope where the fluorophores (fluorescein) inside the droplets are excited by a laser (wavelength 473 nm). Emitted light is collected using a photomultiplier tube (PMT), whose signals are acquired and analyzed by the FPGA card. The chip is also connected to a function generator that provides a sinusoidal voltage (10 kHz, 5 Vp-p) across the electrodes embedded in the chip and the resulting impedance change between the electrodes is analyzed by the FPGA setup after transimpedance amplification (TI). The FPGA also provides a high-voltage pulse for droplet sorting via the high-voltage amplifier (HV-Amp), whenever a sorting event is triggered. The pumps are used to control continuous phase (Q_C) and dispersed phase (Q_D) flow, while the third pump is used to withdraw fluid from the waste channel (Q_W). The direction of data flow, optical path, and fluid flow are depicted by arrows.

(B) Schematic of the microfluidic chip, where gray channels depict the coplanar platinum electrodes for impedance measurements, green channels depict the microfluidic channels in the PDMS for fluid flow, and black channels depict the microfluidic channels for the indium alloy electrodes used for sorting. The connection of each electrode and microfluidic inlets and outlets are also depicted. Zoom-ins show flow-focusing channel for droplet generation, primary impedance electrodes, and sorting junction at the color-coded positions on the left.

(C) Microfluidic chip assembly depicting the PDMS chip on the glass substrate with coplanar electrodes placed on an ITO-coated coverslip. This assembly is then placed into the 3D printed chip holder.

(D) Image of the 3D printed chip holder with the microfluidic chip inside and the conductive copper tape connecting the platinum electrode with ITO coated coverslip for grounding.

See also Figures S1–S3.

Table 1. Control parameters

Parameter	Purpose	Too low	Too high
A_V (pulse amplitude)	defines the strength of dielectrophoretic force required to sort the droplets	not enough dielectrophoretic force to pull the droplet toward collection channel	droplet disruption due to high dielectrophoretic force
D_V (pulse duration)	defines the time span of the sorting pulse required to sort a single droplet	droplet is not pulled long enough to reach collection channel	multiple droplets are pulled along with the correct droplet
L_V (pulse delay)	defines the time delay between droplet detection and sorting trigger to accommodate for the distance between detection zone and sorting junction	may result in sorting of droplets ahead of the correct droplet	may result in sorting of droplets behind the correct droplet
Q_C (continuous phase flow rate)	delivers the continuous phase (oil) to the microfluidic chip	low throughput but high sorting efficiency	high throughput but low sorting efficiency or no sorting
Q_D (dispersed phase flow rate)	delivers the dispersed phase (aqueous) to the microfluidic chip	low throughput with high sorting efficiency	sorting of more than the desired droplet (additional false positives)
Q_W (withdraw flow rate)	withdraws fluid from the waste channel to ensure the default trajectory of every droplet is toward waste channel	some droplets may spontaneously enter in collection channel resulting in false positives	sorting may require higher dielectrophoretic force, resulting in droplet disruption, fusion, and trapping

The purpose of various parameters that iSort optimizes to reach maximum throughput with highest efficiency and the effect of lower or higher than optimum values of these parameters on sorting operation.

experiment, the system is ready with the optimized configurations and can rapidly start the screening. To demonstrate the operation of these modes in detail, we conducted two experiments.

RESULTS

In the first experiment, we used scanning mode to find the highest throughput of a microfluidic chip while sorting every third droplet that passes through the sorting junction. In other words, the algorithm considered every third droplet as the droplet of interest while scanning, so that it would have enough sorting events to quickly iterate through the parameter space. Here, we are considering that sorting a single droplet is an independent event, i.e., the parameters that are found efficient to sort every third droplet should also be equally efficient to sort any single droplet irrespective of its position. We setup the experiment and initiate iSort program as per the instructions in STAR Methods. Once the droplet generation starts at a low throughput (40–50 Hz) and the droplet signals are visible on the iSort interface, we started the scanning mode to find the optimum configuration of control parameters to successfully sort every third droplet (Figure 2A). These parameters, L_V, D_V, and A_V, were optimized by conducting nested iterations with dynamically calculated initial, increment, and maximum values before each iteration cycle (Table S1). During iterations, to ensure the accuracy of droplet sorting (i.e., correctly identifying that the sorted droplet is indeed the droplet of interest), the algorithm has four functionalities: (1) The algorithm started the iterations by gradually increasing L_V and incremented D_V only when the L_V iteration did not reach 100% efficiency (Figure S2). Similarly, A_V was incremented only when D_V iterations were unsuccessful. This sequence allowed efficient sorting at lowest possible values of D_V and A_V preventing sorting of multiple droplets under high D_V or droplet stretch/breaking under high A_V or droplet electrocoalescence[24] if two droplets come close during sorting, which is common at high throughput. (2) The maximum time span of the high-voltage pulse (i.e., $L_V + D_V$) is defined by the spacing between the droplets such that the pulse stops by the time the preceding droplet enters the sorting junction (Table S1). (3) The high-voltage pulse is given a parabolic shape so that as it ends, its amplitude (A_V) is one-third of the maximum amplitude required to pull the droplet. This ensures that even at the maximum pulse duration or if the preceding droplet is closer than the registered spacing (e.g., because of perturbations), the DEP force will not be high enough to deflect the following droplet toward collection channel or merge the two droplets (Figure S3). (4) Whenever a droplet is sorted, it would appear as a peak in the *Z2* signal, and to ensure that this droplet detected by *Z2* was indeed the same droplet that was identified for sorting, the algorithm can continuously estimate the time delay between droplet's identification by fluorescence and its detection by *Z2* (Figure S3). It should also be noted that our method uses FPGA-powered high-speed computation and thus theoretically has the resolution to determine the minimum sorting pulse width down to microseconds, which is at least one order of magnitude

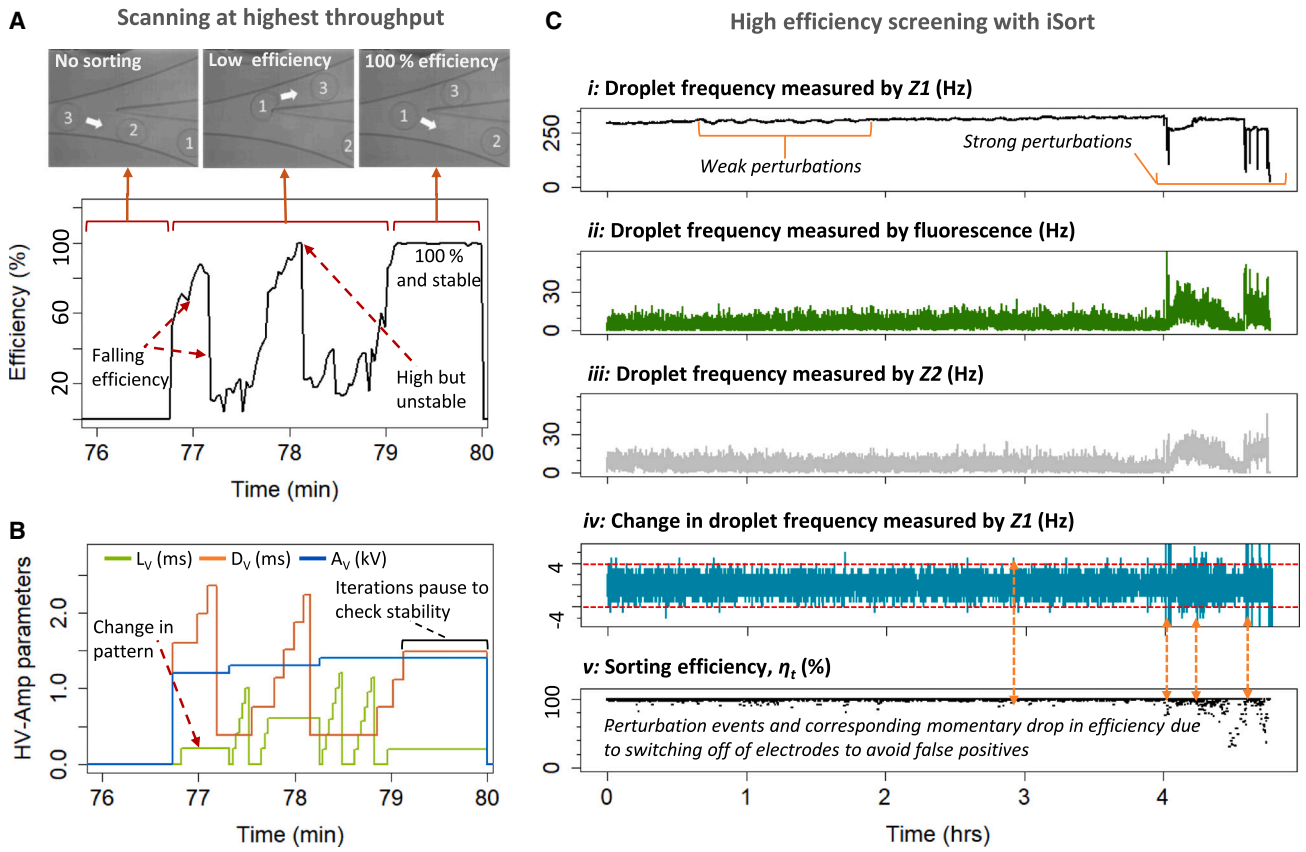

Figure 2. Scanning and screening with iSort

(A) Scanning at a throughput of 320 Hz showing improvement in the sorting efficiency as the iterations proceed along with corresponding images of the microfluidic channels depicting various stages during iterations to reach 100% efficiency while sorting every third droplet (also shown in Video S1). The complete scan from 40 to 320 Hz is shown in Figure S4.

(B) Corresponding iterations of high-voltage parameters to reach 100% sorting efficiency at a throughput of 320 Hz. The change in iteration pattern upon detection of falling efficiency is also highlighted where the L_V iterations stopped before reaching its maximum value and the D_V iterations started. This way, the most optimal parameters can be identified most rapidly, on the basis of a self-correcting algorithm.

(C) Frequency profile of the droplets as measured by different sensors during screening with iSort and the corresponding sorting efficiency. (i) Frequency of all the droplets measured by primary impedance signals (*Z1*). (ii) Frequency of positive droplets (droplets containing green fluorescent beads) measured by fluorescence signals. (iii) Frequency of droplets in the collection channel measured by secondary impedance signals (*Z2*). (iv) The change in frequency (i.e., the difference between the current frequency and the frequency measured one second ago) measured by *Z1* with a threshold (red line) set at ±4 Hz (i.e., >1% of current throughput). This threshold is used by iSort to decide if the perturbations require pausing of the sorting process (i.e., switching off the high-voltage pulse) to avoid false positives and merged droplets. (v) Efficiency (η_t as per Equation 1) of the droplet sorting during the complete screening process. The points at which the efficiency is below 100% are mostly a result of the perturbations and pausing of sorting by iSort upon detection of these perturbations to avoid multiple false positive droplets at the cost of a few true-positive droplets that cause the momentary efficiency drop. A few of such events and the corresponding perturbations are highlighted in the plot with orange arrows.

See also Figures S5 and S6, Video S2, and Table S1.

higher than what is required for droplet sorting (the highest ever achieved throughput in literature used 33 μs pulse duration for a throughput of 30 kHz[25]). Moreover, scanning with such high resolution would drastically increase the scanning time. As a result, the increment step size for L_V and D_V iterations was defined as 10% of the current droplet spacing which considerably reduced the time the algorithm takes to scan for the best configuration (Table S1; Figures 2A, S4, and S5).

Once the iterations began, their progress was continuously monitored by iSort to determine if the iterations were going in right direction. For this, iSort verified how many droplets actually reached the collection channel when 100 droplets were sorted. This way, the efficiency estimation gets a wide dynamic range and its gradual progress can be observed, which is important to have a good control over the iterations. Whenever iSort detected a fall of 5% or higher in the efficiency after updating a particular parameter, the algorithm went back to the previous value of that parameter, skipped the current iteration and started updating the next parameter, thus ensuring the progress achieved so far is not completely wasted (Figure 2B). Numerically, iSort continuously calculates the efficiency (η_t) of the operation by comparing the measured (N_m) and expected (N_E) number of droplets every time the expected count (N_E) equals 100 (Equation 1). N_m is determined by *Z2*, while N_E is the actual

number of droplets sent for sorting after the fluorescence analysis. When $N_E \neq 100$, η_t stays the same as the last registered value (η_{t-1}) (Equation 1).

$$\eta_t = \begin{cases} \left|\frac{(N_m - N_E)}{N_E}\right| & , \quad N_E = 100 \\ \eta_t - 1 & , \quad N_E \neq 100 \end{cases} . \qquad \text{(Equation 1)}$$

As the iterations proceed and η_t reaches 100%, the iterations paused for 1 min, during which the stability of the sorting was observed (Figure 2A). During this pause, if the number of events where η_t was <100% but ≥98% did not exceed 2, the algorithm recorded the configuration of flow rates and high-voltage amplifier parameters at that particular droplet frequency, else the iterations continued to update. In other words, if the droplets are being sorted at 100 Hz, the algorithm allows no more than 4 incorrect sorting events out of 6,000 screened droplets. This tolerance is a necessary real-world approximation to accommodate for the rare disruptive events occurring due to merged droplets or droplets with low spacing (doublets), etc. After saving the configuration, the algorithm increased the droplet frequency by 10 Hz and started iterating the flow rates of continuous and dispersed phase syringe pumps again to generate droplets at the new frequency (50 Hz) via proportional feedback control process (Table S1). The flow rates of the withdraw pump were then iterated in a similar way until all the generated droplets started to go into the waste channel following which, the high-voltage parameters were optimized again and the process continued and repeated itself until it reached the highest throughput of 320 Hz in 80 min beyond which, the efficiency did not reach 100%, even after multiple iterations (Figure S4). An example of one such scanning iteration to reach 100% efficiency at a throughput of 320 Hz and the corresponding efficiency improvement is shown in Figures 2A and 2B and every decision taken by iSort during this scan is described in Figure S5. The corresponding configuration file for each throughput was also generated, which was then used in the next experiment to demonstrate the operation of screening mode (Figure S4).

Finally, to show iSort's capacity to monitor and ensure efficient and long-term sorting using screening mode, we set up a screening experiment that aimed to sort droplets containing fluorescent beads. We replaced the fluorescein syringe from first experiment by another syringe containing a suspension of green fluorescent beads (diameter ~8 μm) and encapsulated these beads into droplets generated on the microfluidic device at an average occupancy of ~0.05 beads per droplet. We uploaded the configuration file from scanning mode and initiated the screening mode on iSort (see STAR Methods for instructions). The algorithm took the suggested values of all parameters from the configuration as initial conditions and initiated the pumps to reach droplet generation at 300 Hz with all droplets going toward the waste channel. The algorithm considered 300 Hz instead of the highest achieved throughput of 320 Hz to keep a margin for flow variation during long-term screens, which otherwise could cause inefficient sorting. The algorithm then started the sorting operation for droplets showing green fluorescence signals of the beads. The screening continued for about 5 h at an average throughput of 307 Hz and an average positive droplet frequency of 6.8 Hz (ranging between 0 and 21 Hz) as measured by fluorescence signals, which also reciprocated with the droplet frequency measured in the collection channel by *Z2,* demonstrating high efficiency (Figure 2C). We observed that for the first 4 h, the flow was relatively stable with a ±16 Hz variation in the throughput, after which the perturbations were strong, probably because of clogging by clustered beads; and by the end of the screen, as the aqueous phase syringe got empty, the throughput gradually decreased and the screening was stopped (Figures 2C and S5). The varying throughput was compensated by the algorithm by correcting the high-voltage parameters in real time in accordance with the configuration file (e.g., if the throughput approached 320 Hz, the algorithm used the A_V, D_V, and L_V values suggested by the configuration file for 320 Hz). Overall, we screened more than 4.2 million droplets until the onset of terminal perturbations, and 114,421 were counted in the collection channel, of which 113,798 were true-positive droplets resulting in a purity (i.e., the fraction of true-positive droplets in the collection) of 99.45% and an enrichment (i.e., the ratio of the fraction of true positives after and before sorting) of 45.8-fold. It should be noted here that the parameters optimized to sort every third droplet have proved to be valid for frequencies of positive droplets ranging from 0 to 21 Hz, confirming our approach of optimizing all parameters under this condition. To support these results, we conducted one more experiment to screen droplets hosting single cells (Mycl-9E10 hybridoma stained with green fluorescent dye), which delivered similar results with 99.52% efficiency and enrichment factor of 46.2 (Figure S6; Video S2; STAR Methods). This high purity is primarily the result of iSort's pausing function, which paused the sorting (i.e., stopped generating the high-voltage pulse) upon detection of perturbations for which the change in the droplet frequency measured by *Z1* was >1% of current throughput (Figure 2C). Pausing the sorting during strong perturbations ensures that the droplets did not encounter any dielectrophoretic force which could have resulted in sorting of multiple negative droplets along with the positive droplets or even merging of droplets because of small spacing in high-throughput screens. This way, pausing aims to prevent large numbers of false positive droplets at the expense of missing a few true positives. To confirm this, we conducted another screen at 300 Hz in similar conditions as above (same chip, same parameters, same droplet size, etc.; Figure S7) in which we first acquired droplet signals with the iSort's pausing function "on" and then with the pausing function "off" (to mimic a conventional screening setup) and found that the conventional screen resulted in higher false positives and merged droplets (11.71%) compared with the screen monitored by iSort (0.72%) (Figures 3A–3C). Even with pausing function, some negative droplets could still enter the collection channel during strong perturbations, preventing the algorithm to reach the ideal 100% purity, nevertheless, iSort successfully reduced such events by at least 16-fold (Figure 3C). We optically analyzed the droplets collected from this experimental screen to further confirm that iSort operated screens deliver higher enrichment with 16.5-fold less false-positive events in comparison with conventional droplet screening setups (Figure 3D).

CellPress
OPEN ACCESS

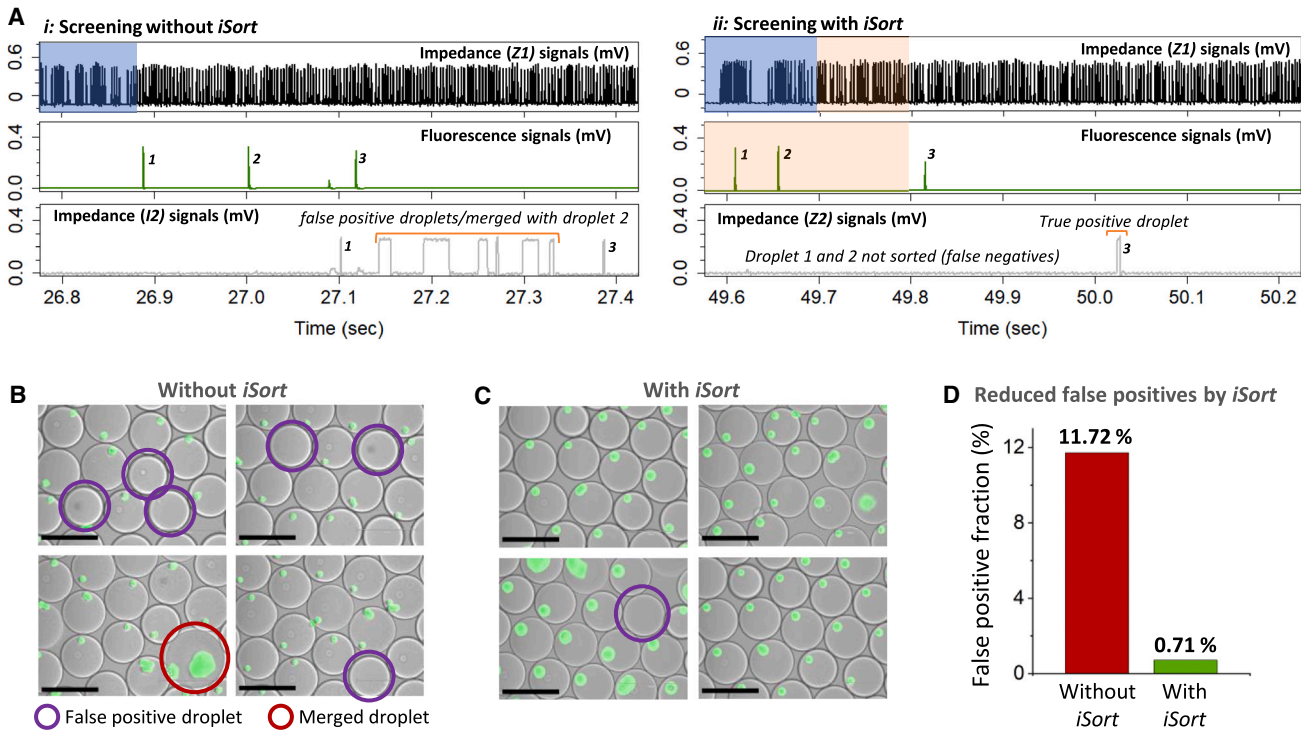

Figure 3. Avoiding false-positive events with iSort

(A) A screening experiment to demonstrate that iSort prevents false-positive events by switching off the electrodes upon perturbations of the system. This enables higher enrichment of true positives in comparison with a conventional screen (screening without iSort), conducted on the same chip under identical conditions. The plots show voltage signals collected from represented sensors where every peak corresponds to a droplet detection (the numbered peaks represent a given droplet detected by different sensors). The perturbations (i.e., the events where the droplet peaks are either bundled or are scattered) are highlighted in blue and the time window where iSort paused the sorting is highlighted in orange. (i) Screening without iSort showing that perturbations cause multiple false positives and merged droplets. (ii) Screening with iSort, showing that iSort paused the sorting operation upon detection of perturbations to avoid false positives.

(B) Images of droplets collected from an iSort operated screen showing few false positives (scale bar: 100 μm).

(C) Images of droplets collected from screen in conventional mode showing multiple false positives and merged droplets.

(D) Comparison of the fraction of false-positive droplets in the collection from the screens operated with and without iSort. The fractions were calculated optically using microscope images of more than 300 droplets.

See also Figure S7.

DISCUSSION

We present a method for optimizing and monitoring the sorting of every single droplet in a microfluidic screen. The system successfully achieves highest throughput and minimizes the collection of false positives to ensure high enrichment factors of true positives. Importantly, all this is done in a fully automated way, enabling untrained people to perform complex droplet sorts. Although we have demonstrated iSort's applicability for the most common droplet screening modality (i.e., FADS),[3,5] its principle of closed feedback control using impedance sensors before and after the sorting event is equally applicable to other microfluidic droplets screening methods that may have a different positive droplet detection modality (absorbance,[26] scattering,[27] impedance,[28] imaging,[29] etc.) or a different sorting actuation approach (acoustic,[30,31] pneumatic valves,[32] thermal,[33] optical tweezer,[34] electrowetting,[35] etc.). We envisage this is a missing piece for enabling broad spreading of single-cell phenotypic analysis, similar to what has been observed for technically less complex single-cell genotypic assays.

Limitations of the study

The provided method is applicable to any screening assay with monodisperse droplet population. For highly polydisperse emulsions the algorithm might not be able to estimate the highest efficiency and throughput of the operation because of variation in droplet velocities inside the channel that sometimes results in droplets bumping into each other and deviating the paths.[3,25] This is demonstrated in Figure S7, where iSort delivered a higher fraction of false positives in the polydisperse droplet screening compared with monodisperse droplet screening. Nevertheless, even with the reduced purity, the fraction of false positives while screening polydisperse population with iSort is still a few folds lower than the false-positive fraction observed while screening monodisperse population without iSort. To reduce false-positive events, iSort identifies the onset of a perturbation and tries to reduce its effect by pausing the sorting. However, as a

perturbation can only be identified once it has already occurred, it may still cause a few false events.

STAR★METHODS

Detailed methods are provided in the online version of this paper and include the following:

- KEY RESOURCES TABLE
- RESOURCE AVAILABILITY
  - Lead contact
  - Materials availability
  - Data and code availability
- EXPERIMENTAL MODEL AND SUBJECT DETAILS
  - Cell lines and culture conditions
- METHOD DETAILS
  - Microfluidic chip fabrication and assembly
  - Electrical connections
  - Experiment setup
  - Initiating iSort
  - Conducting scanning experiment
  - Conducting screening experiment
  - Fluorescent beads suspension preparation
  - Single cell staining and encapsulation
- QUANTIFICATION AND STATISTICAL ANALYSIS

SUPPLEMENTAL INFORMATION

Supplemental information can be found online at https://doi.org/10.1016/j.crmeth.2023.100478.

ACKNOWLEDGMENTS

Parts of this work were supported by DFG grant ME 3536/9-1. We thank Christian Kieser from Electronics Workshop, European Molecular Biology Lab (EMBL), Heidelberg, Germany, for useful discussions and fabrication of the transimpedance amplifier circuit. We also thank Dr. A. Autour from Laboratory of BioMedical Microfluidics, École Polytechnique Fédérale de Lausanne (EPFL), for generously providing the stained cell suspension.

AUTHOR CONTRIBUTIONS

C.A.M. conceived the project and supervised the experimental work. J.P. introduced the impedance analysis-based automation algorithm and conducted experiments. J.P., R.U., L.F., and D.F. wrote the LabVIEW script for the iSort program. J.P. and C.A.M. wrote the manuscript.

DECLARATION OF INTERESTS

Parts of the technology described here have been patented. If the patents are ever licensed, the authors might profit financially though the inventor reward programs of the involved institutes.

INCLUSION AND DIVERSITY

We support inclusive, diverse, and equitable conduct of research.

Received: December 16, 2022
Revised: March 24, 2023
Accepted: April 18, 2023
Published: May 12, 2023

REFERENCES

1. Carnero, A. (2006). High throughput screening in drug discovery. Clin. Transl. Oncol. *8*, 482–490. https://doi.org/10.1007/s12094-006-0048-2.
2. Herzenberg, L.A., Sweet, R.G., and Herzenberg, L.A. (1976). Fluorescence-activated cell sorting. Sci. Am. *234*, 108–117. https://doi.org/10.1038/scientificamerican0376-108.
3. Baret, J.-C., Miller, O.J., Taly, V., Ryckelynck, M., El-Harrak, A., Frenz, L., Rick, C., Samuels, M.L., Hutchison, J.B., Agresti, J.J., et al. (2009). Fluorescence-activated droplet sorting (FADS): efficient microfluidic cell sorting based on enzymatic activity. Lab Chip *9*, 1850–1858. https://doi.org/10.1039/B902504A.
4. Mazutis, L., Gilbert, J., Ung, W.L., Weitz, D.A., Griffiths, A.D., and Heyman, J.A. (2013). Single-cell analysis and sorting using droplet-based microfluidics. Nat. Protoc. *8*, 870–891. https://doi.org/10.1038/nprot.2013.046.
5. Panwar, J., Autour, A., and Merten, C.A. (2023). Design and construction of a microfluidics workstation for high-throughput multi-wavelength fluorescence and transmittance activated droplet analysis and sorting. Nat. Protoc. *18*, 1090–1136. https://doi.org/10.1038/s41596-022-00796-2.
6. Wang, Y., Jin, R., Shen, B., Li, N., Zhou, H., Wang, W., Zhao, Y., Huang, M., Fang, P., Wang, S., et al. (2021). High-throughput functional screening for next-generation cancer immunotherapy using droplet-based microfluidics. Sci. Adv. *7*, eabe3839. https://doi.org/10.1126/sciadv.abe3839.
7. Colin, P.-Y., Kintses, B., Gielen, F., Miton, C.M., Fischer, G., Mohamed, M.F., Hyvönen, M., Morgavi, D.P., Janssen, D.B., and Hollfelder, F. (2015). Ultrahigh-throughput discovery of promiscuous enzymes by picodroplet functional metagenomics. Nat. Commun. *6*, 10008. https://doi.org/10.1038/ncomms10008.
8. Abatemarco, J., Sarhan, M.F., Wagner, J.M., Lin, J.-L., Liu, L., Hassouneh, W., Yuan, S.-F., Alper, H.S., and Abate, A.R. (2017). RNA-aptamers-in-droplets (RAPID) high-throughput screening for secretory phenotypes. Nat. Commun. *8*, 332. https://doi.org/10.1038/s41467-017-00425-7.
9. El Debs, B., Utharala, R., Balyasnikova, I.V., Griffiths, A.D., and Merten, C.A. (2012). Functional single-cell hybridoma screening using droplet-based microfluidics. Proc. Natl. Acad. Sci. USA *109*, 11570–11575. https://doi.org/10.1073/pnas.1204514109.
10. Gérard, A., Woolfe, A., Mottet, G., Reichen, M., Castrillon, C., Menrath, V., Ellouze, S., Poitou, A., Doineau, R., Briseno-Roa, L., et al. (2020). High-throughput single-cell activity-based screening and sequencing of antibodies using droplet microfluidics. Nat. Biotechnol. *38*, 715–721. https://doi.org/10.1038/s41587-020-0466-7.
11. Ahn, K., Kerbage, C., Hunt, T.P., Westervelt, R.M., Link, D.R., and Weitz, D.A. (2006). Dielectrophoretic manipulation of drops for high-speed microfluidic sorting devices. Appl. Phys. Lett. *88*, 024104. https://doi.org/10.1063/1.2164911.
12. Gawad, S., Schild, L., and Renaud, P.H. (2001). Micromachined impedance spectroscopy flow cytometer for cell analysis and particle sizing. Lab Chip *1*, 76–82. https://doi.org/10.1039/B103933B.
13. Morgan, H., Sun, T., Holmes, D., Gawad, S., and Green, N.G. (2006). Single cell dielectric spectroscopy. J. Phys. D Appl. Phys. *40*, 61–70. https://doi.org/10.1088/0022-3727/40/1/S10.
14. Spencer, D., and Morgan, H. (2020). High-speed single-cell dielectric spectroscopy. ACS Sens. *5*, 423–430. https://doi.org/10.1021/acssensors.9b02119.
15. Honrado, C., Bisegna, P., Swami, N.S., and Caselli, F. (2021). Single-cell microfluidic impedance cytometry: from raw signals to cell phenotypes using data analytics. Lab Chip *21*, 22–54. https://doi.org/10.1039/D0LC00840K.
16. Chawla, K., Modena, M.M., Ravaynia, P.S., Lombardo, F.C., Leonhardt, M., Panic, G., Bürgel, S.C., Keiser, J., and Hierlemann, A. (2018). Impedance-based microfluidic assay for automated antischistosomal drug screening. ACS Sens. *3*, 2613–2620. https://doi.org/10.1021/acssensors.8b01027.

17. Panwar, J., and Roy, R. (2019). Integrated Field's metal microelectrodes based microfluidic impedance cytometry for cell-in-droplet quantification. Microelectron. Eng. *215*, 111010. https://doi.org/10.1016/j.mee.2019.111010.

18. Yakdi, N.E., Huet, F., and Ngo, K. (2016). Detection and sizing of single droplets flowing in a lab-on-a-chip device by measuring impedance fluctuations. Sensor. Actuator. B Chem. *236*, 794–804. https://doi.org/10.1016/j.snb.2016.05.123.

19. Fan, W., Chen, X., Ge, Y., Jin, Y., Jin, Q., and Zhao, J. (2019). Single-cell impedance analysis of osteogenic differentiation by droplet-based microfluidics. Biosens. Bioelectron. *145*, 111730. https://doi.org/10.1016/j.bios.2019.111730.

20. Fan, W., Xiong, Q., Ge, Y., Liu, T., Zeng, S., and Zhao, J. (2022). Identifying the grade of bladder cancer cells using microfluidic chips based on impedance. Analyst *147*, 1722–1729. https://doi.org/10.1039/D2AN00026A.

21. Chen, J., Xue, C., Zhao, Y., Chen, D., Wu, M.-H., and Wang, J. (2015). Microfluidic impedance flow cytometry enabling high-throughput single-cell electrical property characterization. Int. J. Mol. Sci. *16*, 9804–9830. https://doi.org/10.3390/ijms16059804.

22. Zaborowski, M., Grabiec, P., and Barcz, A. (2005). Manufacturing of Pt-electrode by wet etching. Microelectron. Eng. *82*, 283–288. https://doi.org/10.1016/j.mee.2005.07.036.

23. Pryszlak, A., Wenzel, T., Seitz, K.W., Hildebrand, F., Kartal, E., Cosenza, M.R., Benes, V., Bork, P., and Merten, C.A. (2022). Enrichment of gut microbiome strains for cultivation-free genome sequencing using droplet microfluidics. Cell Rep. Methods *2*, 100137. https://doi.org/10.1016/j.crmeth.2021.100137.

24. Priest, C., Herminghaus, S., and Seemann, R. (2006). Controlled electrocoalescence in microfluidics: targeting a single lamella. Appl. Phys. Lett. *89*, 134101. https://doi.org/10.1063/1.2357039.

25. Sciambi, A., and Abate, A.R. (2015). Accurate microfluidic sorting of droplets at 30 kHz. Lab Chip *15*, 47–51. https://doi.org/10.1039/C4LC01194E.

26. Gielen, F., Hours, R., Emond, S., Fischlechner, M., Schell, U., and Hollfelder, F. (2016). Ultrahigh-throughput–directed enzyme evolution by absorbance-activated droplet sorting (AADS). Proc. Natl. Acad. Sci. USA *113*, E7383–E7389. https://doi.org/10.1073/pnas.1606927113.

27. Wang, X., Ren, L., Su, Y., Ji, Y., Liu, Y., Li, C., Li, X., Zhang, Y., Wang, W., Hu, Q., et al. (2017). Raman-activated droplet sorting (RADS) for label-free high-throughput screening of microalgal single-cells. Anal. Chem. *89*, 12569–12577. https://doi.org/10.1021/acs.analchem.7b03884.

28. Kemna, E.W.M., Segerink, L.I., Wolbers, F., Vermes, I., and van den Berg, A. (2013). Label-free, high-throughput, electrical detection of cells in droplets. Analyst *138*, 4585–4592. https://doi.org/10.1039/C3AN00569K.

29. Sesen, M., and Whyte, G. (2020). Image-based single cell sorting automation in droplet microfluidics. Sci. Rep. *10*, 8736. https://doi.org/10.1038/s41598-020-65483-2.

30. Zhong, R., Yang, S., Ugolini, G.S., Naquin, T., Zhang, J., Yang, K., Xia, J., Konry, T., and Huang, T.J. (2021). Acoustofluidic droplet sorter based on single phase focused transducers. Small *17*, 2103848. https://doi.org/10.1002/smll.202103848.

31. Li, S., Ding, X., Guo, F., Chen, Y., Lapsley, M.I., Lin, S.-C.S., Wang, L., McCoy, J.P., Cameron, C.E., and Huang, T.J. (2013). An on-chip, multichannel droplet sorter using standing surface acoustic waves. Anal. Chem. *85*, 5468–5474. https://doi.org/10.1021/ac400548d.

32. Zhou, Y., Yu, Z., Wu, M., Lan, Y., Jia, C., and Zhao, J. (2023). Single-cell sorting using integrated pneumatic valve droplet microfluidic chip. Talanta *253*, 124044. https://doi.org/10.1016/j.talanta.2022.124044.

33. Robert de Saint Vincent, M., Wunenburger, R., and Delville, J.-P. (2008). Laser switching and sorting for high speed digital microfluidics. Appl. Phys. Lett. *92*, 154105. https://doi.org/10.1063/1.2911913.

34. Zhao, Z., Xia, J., Huang, T.J., and Zou, J. (2022). Ring-shaped photoacoustic tweezers for single particle manipulation. Opt. Lett. *47*, 826–829. https://doi.org/10.1364/OL.447861.

35. Chen, Y., and Wang, S. (2018). Development of coplanar electro-wetting based microfluidic sorter to select micro-particles in high volume throughput at milliliter amount within twenty minutes. Sensors *18*, 2941. https://doi.org/10.3390/s18092941.

36. Zeng, W., Xiang, D., and Fu, H. (2019). Prediction of droplet production speed by measuring the droplet spacing fluctuations in a flow-focusing microdroplet generator. Micromachines *10*, 812. https://doi.org/10.3390/mi10120812.

STAR★METHODS

KEY RESOURCES TABLE

REAGENT or RESOURCE	SOURCE	IDENTIFIER
Deposited data		
Raw Data from scanning and screening results	This paper	Zenodo Database: https://doi.org/10.5281/zenodo.7357839
Software and algorithms		
iSort Software	This paper	Zenodo Database: https://doi.org/10.5281/zenodo.7437748
LabVIEW 2016 or higher, full or run-time Engine, 32-bit	National Instruments	https://www.ni.com/
LabVIEW FPGA Module 2016 0r higher, 32-bit	National Instruments	https://www.ni.com/
NI R series Multifunction RIO Device drivers	National Instruments	https://www.ni.com/
Experimental models: Cell lines		
Mycl-9E10 Hybridoma cells	ECACC	Cat # 85102202; RRID: CVCL_L708
Other		
Conventional droplet sorting setup	Panwar et al. 2023[5]	
CAD files to fabricate microfluidic chip	This paper	Zenodo Database: https://doi.org/10.5281/zenodo.7357839
STL file to 3D print the chip holder	This paper	Zenodo Database: https://doi.org/10.5281/zenodo.7357839
FPGA card, PXIe-7856R	National Instruments	Cat# 784145-01
PTFE tubing	Adtech	Cat# TW30
Polydimethylsiloxane (PDMS) + Crosslinker Kit	Dow Corning	Sylgard 184
Negative photoresist	Microchem	SU8 2075
Positive photoresist	Microchem	AZ 10XT
Photomask or 5 in Chrome mask	Selba S.A.	https://selba.ch/
4-inch Silicon wafer	Siltronix	100/P/SS/0.1-100
4-inch Glass wafer	Swift Glass	Borofloat 4in/100mm
Biopsy punch 0.75 mm and 0.5 mm	ProSciTech	Cat# T983-07/05
Indium Alloy wire	Indium Corporation	Wire dia: 0.5 mm with 51 % In, 32% Bi and 16.5 % Sn
Spring contact	Distrelec	Cat# 14022286
Indium Tim Oxide (ITO) coated glass slide (50 mm x 70 mm x 1.1 mm)	Diamond coating	Float Glass with 8-12 Ohm/m^2 ITO
Function generator (2-channel)	Techtronix	Cat# AFG1062
Power supply (2-channel, ± 5 V, 2 Amp)	Distrelec	Cat# RND320KD3305P
Syringe pumps	Harward Apparatus	Cat# 70-3007
Syringe: 10ml, 3 ml		
Syringe needle: 27G		
PTFE Tubing (0.3 mm ID, 0.5 mm OD)	Adtech Polymer Engg.	Cat# TW30
Conductive tape (Copper)	3M	Cat# 1181X1/4
Syringe filter, 0.22 μm	Millex	Cat# SLGSV255F
Magnetic bead	VWR	Cat# 4420364
Magnetic stirrer bar	Heidolph Instruments	Cat# 5030200000
Countess II, Automatic cell counter	Thermo Fisher Sc.	Cat# AMQAX1000
Novec™ 7500 oil	3M	Cat# 98-0212-29285

(*Continued on next page*)

Continued

REAGENT or RESOURCE	SOURCE	IDENTIFIER
PicoSurf (5% (wt/wt)	SphereFluidics	Cat# C022
Aquapel Treatment tube	Autoserve gmbh	Cat# A001
Fluorescein sodium salt	Sigma-Aldrich	Cat# 46960
Phosphate Buffered Saline (PBS) pH 7.4	Gibco	Cat# 10010-015
PolyStyrene/Dragon Green Fluorescent Bead	Bangs Laboratories	Cat# FSDG007
Calcein AM Viability Dye (UltraPure Grade)	Invitrogen	Cat# 65-0853-39
RPMI media	Gibco	Cat# 61870036

RESOURCE AVAILABILITY

Lead contact

Further information and requests for resources and reagents should be directed to and will be fulfilled by the Lead Contact, Christoph A. Merten:christoph.merten@epfl.ch (updates can be found on lab's webpage: www.epfl.ch/labs/lbmm/downloads/).

Materials availability

The CAD file for the microfluidic chip design and the STL file to 3D print the chip holder can be downloaded from Zenodo Database: https://doi.org/10.5281/zenodo.7357839. Circuit for transimpedance amplifier can be provided upon request to lead contact.

Data and code availability

- Datasets associated with this paper are freely available at Zenodo Database: https://doi.org/10.5281/zenodo.7357839.
- The complete iSort program is freely available at Zenodo Database: https://doi.org/10.5281/zenodo.7437748.
- Any additional information required to reanalyze the data reported in this paper is available from the lead contact upon request.

EXPERIMENTAL MODEL AND SUBJECT DETAILS

This study proposes a method to automate a conventional fluorescence activated droplet sorting platform[4,5,9] using impedance analysis as discussed below to conduct highly efficient long-term droplet screening at highest throughput and robustness. The additional hardware and software necessary to implement the method can be accessed from the provided links.

Cell lines and culture conditions

To demonstrate our methods capacity to conduct high-throughput droplet screening for single cell analysis, we sorted droplets hosting single Mycl-9E10 hybridoma cells obtained from the European Collection of Authenticated Cell Cultures (ECACC, UK). These cells were cultured in RPMI media (Gibco) in 5% CO_2 atmosphere at 37°C in humidified conditions. The cell suspension we used had a viability of 81% with a density of 3.73 x 10^6 cells per mL as measured using automatic cell counter. These cells were then stained and encapsulated in droplets as discussed below.

METHOD DETAILS

Microfluidic chip fabrication and assembly

The complete microfluidic chip was comprised of two layers, the top layer was made of Polydimethylsiloxane (PDMS) that had microfluidic channels on it and the bottom layer was the electrode layer made by depositing platinum on a glass wafer (Figures 1B and S1). First, the provided CAD files were used to etch the pattern for the microfluidic channels and electrodes on two separate chrome masks using Laser lithography (Heidelberg VPG200). For the top layer, 50 μm thick layer of negative photoresist (Microchem SU8 2075) was deposited on a silicon wafer which was then exposed to UV radiation through its respective chrome mask using a mask aligner and exposure tool (Süss MJB4) and then developed. PDMS (mixed with crosslinker in 10:1 ratio) was poured on this silicon wafer and then kept at 80°C for 1 h to generate ∼5mm thick PDMS chip with microchannels. Inlets and outlets for fluid were made using a 0.75 mm biopsy punch and for sorting electrodes using a 0.5 mm biopsy punch (shown in black in Figure 1B).

For electrode layer, 20 nm Titanium and 200 nm Platinum were sequentially deposited on a glass wafer using metal sputtering (Spider 600).[12,22] Following this, a 2 μm thick layer of positive photoresist was spun coated the wafer. After UV exposure and development, the exposed metal (Ti/Pt) was etched away using ion-beam etching (Nexus IBE 350). After etching, the wafer looked transparent with only the electrode pattern covered with the photoresist which was then removed chemically resulting into a glass wafer with metal electrodes patterned on it. The wafer was then diced into 35 mm x 25 mm wafers with electrodes. The PDMS chip was then

plasma bonded on the electrode wafer using the guide marks to align. To generate the 3D electrodes used for sorting, the microfluidic chip was first placed on a hotplate at 95°C for 10 min. The 1 cm long fragment of the Indium Alloy wire was inserted into the inlets of the microchannel dedicated for electrodes (shown in black in Figure 1B) and pushed using a tweezer till it melts and comes out of the other end of the channel.[5] Repeat the same steps for the secondary electrodes and keep the chip at room temperature till the alloy solidifies. For hydrophobic treatment of the microchannels, we passed Aquapel through the microfluidic channels via a 0.22 μm syringe filter and flushed the channels with HFE 7500 oil after a rest of 10 seconds. Place an ITO coated slide under the chip such that the coated side points outwards and fix them using a 5 mm fragment of the double-sided conductive tape on the ground ports (Figures 1C and S1).[5] We 3D-printed the chip-holder using the provided STL file and glued the spring contacts in all its 1mm holes such that the contact pins points downwards and soldered wires on its other end (Figure 1D). We then placed the microfluidic chip in the holder and fixed the assembly using the screws.

Electrical connections

First the microfluidic chip and holder assembly was placed on the microscope stage such that its brightfield image was visible through the camera via a 40x objective. Two reference signals (from the function generator) of 10 kHz and 8 V peak to peak voltage, each, were then connected to their respective ports on the microfluidic chip (Figures 1B and S1). Subsequently, the high voltage wires were connected to the sorting electrodes (shown in black in Figure 1B). Then the input wires from the transimpedance amplifier (TI-Amp) were connected to their dedicated ports on the chip (Figures 1B and S1) and the output wires from TI-amp were also connected to the analog input ports of the FPGA card (AI03 and AI04 respectively as per the provided iSort software). Finally, the transimpedance amplifier circuit was provided with ± 5 V DC using a 2-channel power supply.

Experiment setup

Two 10 mL syringes containing dispersed (PBS with 100 μM Fluorescein) and continuous phase (HFE 7500 oil + 1 % Picosurf) were placed in separate syringe pumps and were connected with their respective inlets in the microfluidic chip via ~20 cm PTFE tubing. The microchannels were first primed flowing oil at the flowrate of ~25 μl/hr (For best results, the dispersed phase fluid during scanning should be same as dispersed phase fluid to be used in actual screening). One more syringe containing continuous phase was inserted in another syringe pump at a flow rate of ~15 μl/hr. This syringe was connected to the waste outlet of the chip via a tubing such that there was no trapped air in the tube or syringe or chip. A short tube was also connected to the collection outlet of the chip with its other end in a collection vial. The setup was allowed to run for ~15 min or till the collection tube started to fill. Then the inlet flowrates of continuous (Q_C) and dispersed (Q_D) phase were changed to 400 μl/hr and 40 μl/hr respectively and the withdraw flowrate (Q_W) of the syringe pump in waste outlet was changed to 300 μl/hr. The low flow rate ratio (Q_D/Q_C) ensured a high spacing between the droplets[36] which is necessary for efficient high-throughput screening.[3] The three syringe pumps were connected to the PC via USB and their respective serial port numbers were noted (The serial port numbers or COM ports for each pump were checked on PC's device manager). The pumps were left running till the droplets started to generate.

Initiating iSort

First, the FPGA model and the analog input (AI) ports for the photomultiplier tubes (PMT) and Impedance sensors (IMP) were selected in the *communication tab* of the iSort software (Figure S8). The provided iSort software version can accommodate up to three PMTs with default values as AI0 to AI2 for PMT1 to PMT3, however, as the scanning needed just one PMT, the other PMTs were set to *off*. Similarly, the default ports for primary and secondary impedance sensors were set to AI3 and AI4 respectively. Subsequently, the serial ports (COM port) numbers for the three syringe pumps were selected in the *communication tab*. The rest of the inputs were set to their default values. After these inputs, the iSort program was initiated by clicking on the arrow button on top right (Figure S8). Then the *start pumps* toggle was clicked to connect the pumps with the program. Then the PMTs, function generator and the power supply along with the laser to excite the fluorescein in the droplets were turned on and the microfluidic chip was also repositioned on the stage such that the laser was focused at the center of the detection zone before the sorting junction[5](Figure 1B). The Live Data plot on the iSort interface showed some signals from the primary and secondary Impedance sensors where every peak represented a droplet passing over the electrode array (Figures S1 and S8). The Live Data plot also showed some faint droplet signals from the PMT which were made stronger by turning up the PMT gain (Figure S8). A gain value between 0.4 V to 0.45 V was sufficient to see clear droplet fluorescence peaks. To let iSort identify the droplets from each sensor, the thresholding cursor was moved such that the droplet peaks cross the cursor (Figure S8). From here, iSort could either be used in *scanning* or in *screening* modes.

Conducting scanning experiment

This mode was used to scan the control parameters and obtain the most optimum configuration of these parameters at the highest throughput for that particular microfluidic device. A target droplet frequency as 50 Hz was inserted in the iteration tab (This target frequency was taken as the minimum frequency to start the scanning, for best results, this should be set at a value higher than the current droplet frequency which can be found in the top middle plot). All the droplets in the gating tab were selected for both fluorescence and impedance signals (Figure S8). Select A *test ratio* as 3:1 was selected, the *Scan* toggle was turned *on* and then *Autopilot* was clicked. This way, the algorithm was initiated which ran till the highest throughput was obtained beyond which, a 100% sorting efficiency could not be reached. A configuration file was generated and saved for later use (Figure S4).

Conducting screening experiment

This mode was used to conduct long-term screening at the most optimum and highest throughput as suggested by the configuration file. Once the experiment was setup and the droplets were visible at the sorting junction, the threshold on the droplet fluorescence signals in the Live data window was set and the droplets to be sorted were selected in the gating window (Figure S8). The desired configuration file was loaded by clicking on *Load* button and the *Screen* toggle was turned *on*. Finally, the *Autopilot* button was clicked. The algorithm first updated the fluid flow rates to reach the suggested throughput and then updated the high-voltage parameters to start screening. The algorithm also consistently monitored the screening to ensure highest sorting efficiency (Figures 3 and S8).

Fluorescent beads suspension preparation

150 μL of Dragon green fluorescent bead stock was added to 1850 μL of PBS to reach an average occupancy of 0.05 beads per droplet. Then this solution was filled into a 3 mL syringe (with 27G needle) along with a magnetic stirring bar and a ∼20 cm long PTFE tubing was inserted into the needle using a tweezer. During the experiment, this syringe was placed into the syringe pump and a magnetic stirrer set at 500 rpm was positioned close to the top of this syringe such that the magnetic stirring bar started mixing the bead suspension, which ensured that the beads stayed un-clustered and suspended in the syringe.

Single cell staining and encapsulation

Prior to sorting experiments, Mycl-9E10 hybridoma cells were pelleted from a suspension at 200 g for 5 min. After removing the supernatant, the cells were resuspended into 2 mL in PBS, pre-warmed at 37°C. Subsequently 2 μL of Calcein AM viability dye (10 mM) were added, before incubating the suspension for 20 min at 37°C in a 5% CO_2 atmosphere. We then washed the cells twice prior to pelleting and resuspending in 1mL PBS. Cell density was determined using an automatic cell counter and adjusted to match an average occupancy of ∼0.02 cells per ∼200 pl droplet (corresponding to a concentration of $\sim 10^6$ cells per mL). 2 mL of the cell suspension was then filled into a 3 mL syringe along with a magnetic stirring bar. The syringe was connected to a ∼20 cm long PTFE tubing and placed into the syringe pump close to a magnetic stirrer to agitate cells and prevent settling at the bottom of the syringe. The PTFE tubing was then inserted into the aqueous phase inlet of the microfluidic chip as discussed above in experiment setup.

QUANTIFICATION AND STATISTICAL ANALYSIS

Optical analysis is done using microscope images. Exact n values are described in the relevant figure legends and the error bars represent the standard deviation around mean. Signal processing including droplet fluorescence and impedance analysis is done in real-time by the provided software and the post experiment data analysis was done using custom scripts in R.